A Study on the Flow Field Characteristics of Air Induction System for Reducing the Signal-to-Noise in the MAFS Output

Seoung-Chool Yoo *

ABSTRACT

This study presents the flow visualization results, velocity and turbulence intensity measurements made within an air filter cover and entry region of a mass air flow sensor (MAFS) which is used in an induction system of 3.8L engine. Flow structure in two air filter cover assemblies were examined. The first was a clear plastic replica of the production cover while the second was a modified clear plastic cover with a geometry configured to reduce fluctuations. High speed flow visualization and laser doppler velocimetry (LDV) systems were used to reveal and analyze the flow field characteristics encountered in the sensor design process under steady flow conditions. A 40-watt copper vapor laser was used as a light source. Its beam is focused down to a sheet of light approximately 1.5mm thick. The light scattered off the particles was recorded by a 16mm high speed rotating prism camera at 5000 frames per second.

A comparison of the flow patterns and LDV measurements in the original and modified air filter covers is presented to illustrate the controlling effect of the cover design on the turbulence structure formation near the bypass and on the sensor output signal. In both axial and radial planes of the main passage it was found that the turbulence flow pattern is remarkably influenced by the air filter cover and main passage configuration.

Keywords: mass air flow sensor (MAFS), LDV, high speed flow visualization, copper vapor laser, air induction system.

INTRODUCTION

With the recent advances in internal combustion engines and engine electronic control functions, new technologies of mass air flow sensor (MAFS) monitoring are directed toward improving fuel economy, performance and exhaust emissions of undesirable pollutants which depend largely on the fuel-air mixture formation process[1,2,3,4,5]. An accurate, high response MAFS provides optimum engine control over a wide operating range. Despite the advantages of the MAFS over the manifold absolute pressure sensor, the instabilities in the output signal at low flow rates raised a major concern in employing the MAFS in the market on a larger basis[4,5]. The purpose of this investigation is to analyze the flow structure and the controlling parameters which influence the air flow in the entrance region of the MAFS.

Disturbances in the MAFS output signal is due to micro-scale turbulence structures generated at the surface of the hot-wire probe. This is a result of the interaction between the complex velocity and the temperature field at the sensor element. By controlling the flow field near the sensor it is possible to reduce the noise and enhance the sensor performance over a wide range of mass flow rates[5]. In this respect, the ability to predict a successful design of a MAFS depends typically on a more comprehensive study of the influencing parameters, namely, the air filter

* Halla Institute of Technology

cover and the bypass inlet design required to maintain a careful ducting of the airflow approaching the meter. A good bypass inlet design can reduce the instabilities of the velocity field flowing through the bypass passage. The subsequent reduction of micro-scale turbulence structures on the active surface of the hot-wire probe will provide improved control systems. It is evident that detailed analytical and experimental studies which illustrate how the controlling parameters influence the sensor are required to develop the knowledge about the relevant flow characteristics. In particular the flow structure near the MAFS bypass passage which has a great impact on the system performance. This will ensure that new concepts are adequately assessed for feasibility and successful design at an early stage of the process.

The capability to build and test practical bypass inlet designs have been developed. These inlets are intended to reduce entry losses/noise in the MAFS output during idling, and in an economical way, improve performance and long-term reliability. In this research, details of the flow characteristics are described under steady flow conditions. Air flow within the air filter cover and in the entrance region of the MAFS is characterized by using high speed flow visualization technique and laser doppler velocimetry (LDV). The visual observations have provided valuable information about the flow field and are used to interpret the LDV velocity and turbulence intensity measurements.

EXPERIMENTAL TECHNIQUES AND FACILITIES

Flow Visualization System

The high speed flow visualization system used for this study is shown in Figure 1. It consists of a 40 watt copper vapor laser (CVL), mirrors, cylindrical lenses, a high speed camera, a particle generator and a synchronization timing system.

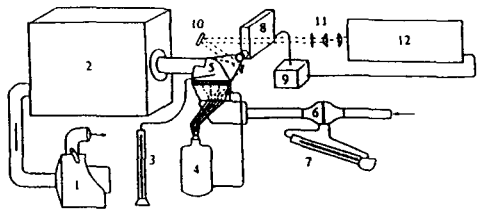

Fig. 1 Air flow visualization system and experimental setup. (1. Centrifugal blower with throttle 2. Plenum 3. Manometer 4. Smoke generator 5. Air induction system 6. Laminar air flow element 7. Inclined manometer 8. High speed camera 9. Synchronization timing system 10. Mirrors 11. Cylindrical lenses 12. Copper vapor laser)

The CVL Model 451 is well suited as a light source for high speed visual techniques. It is a gas discharge device of 40 watt average output power manufactured by Metalaser Technologies. It emits short pulses at repetition rates of 5000 pulses per second (pps) and a pulse energy of 8 mJ in the green and yellow regions of the visible spectrum, at wavelengths of 510 and 578 nm. The pulse rate can vary between 4000-6000 pps for efficient laser operation. The pulse width is approximately 30 ns and pulse jitter is 3 ns. The driver can be operated using the internal 5 khz oscillator or by applying the external pulse to the trigger select.

The laser beam (5.08 cm in diameter and having a Gaussian power distribution) is directed toward the air cleaner cover and the MAFS unit by a set of three circular mirrors whose diameters are 10.16 cm. These mirrors together provide high-resolution angular control with coplanar-orthogonal adjustments. A cylindrical lens 10.16 cm square, 2.54 cm thick, made of BK-7 optical quartz and one cylindrical mirror were used to focus the beam into a light sheet approximately 1.5 mm thick. Their focal lengths are 332 cm and 20 cm respectively. This laser light sheet provides enough exposure to the films

used for the high speed flow visualization.

A 16 mm NAC E-10/EE high speed rotating prism camera which offers a fast f 2.5 optical system is used to film flow images on a negative Kodak film (7292 tungsten, 320 ASA, 2-stops push processed to 1600 ASA). The camera is equipped with a trigger pulse generator and optical pick-up to trigger the CVL at 5 khz and synchronize the laser pulses with the film frame rate at 5000 frames per second (fps).

An electronic timing system was designed and built specifically to switch the thyratron driver of the CVL from internal to external mode. In the external mode the pulse generator of the camera triggers the laser during the filming process. At the end of the film the timing control switches the laser back to the internal mode. Also, the synchronization system can be used to control the operation of the solenoid valve for a preset number of crank angles. A more detailed description of the procedure and the electronic timing system is given in Reference 6.

Laser Doppler Velocimetry System

Quantitative flow analysis is very important in describing flow phenomena. Although the high speed flow visualization shows important information for qualitative analysis, it does not provide the quantitative information needed to specify local flow fields. The velocities in several planes, based on examination of the high speed flow visualization films, were measured by a two-component LDV. Laser velocimetry is a non-intrusive flow measurement technique. It provides a complete quantitative measurements of the velocity components independent of temperature, density and composition changes in the fluids. The LDV system consists of a 4 watts Ar-ion laser, optics, receiving optics, digital burst correlator (IFA 750), traverse mechanism, and computer. A multi-wavelength beam emitted from an Ar-ion laser is used as a light source. The multi-wavelength beam is separated into several single wavelength beams by a prism. Two wavelengths (488 nm and 514.5 nm) are then selected to measure two velocity components. Receiving optics are used to detect doppler signals scattered by particles in the measuring volume created by the laser beams. These doppler signals are analyzed by a digital burst correlator to calculate the two velocity components at the location of the measuring volume.

To measure two velocity components, four parallel beams were focused at the measuring point on the face of the plane. Two blue beams (488 nm) were focused for u-component measurement and two green beams (514.5 nm) were used for v-component measurement. Two bragg cell frequency shifters were installed to measure negative velocities. The principle characteristics of the optical system are given in Table 1.

Table 1. Optical system characteristics

Characteristics	
half angle	blue: 4.9 ° green:4.9 °
fringe spacing	blue: 2.8 μm green: 3.0 μm
number of fringes	blue: 53 green: 53
volume - blue	d_m: 0.15 mm l_m: 1.8 mm
volume - green	d_m: 0.15 mm l_m: 1.7 mm
laser power	2 W
frequency shift	5 or 10 Mhz
operating mode	coincidence
sampling time	200 μs
coincidence window width	2 μs
data rate	2000

Since LDV measures the velocity of the particles in the flow, it is important to select the particles that follow the fluid flow and have a

large refractive index at the wavelength used for the measurement. For this purpose, a Six-Jet Atomizer (TSI, Model 9306) was used for atomizing the mixture of propylene glycol and water as scattering particles. This atomizer generates particles in the range of 0.3 to 0.8 μm.

The forward scattering doppler signals from the seed particles are detected by photomultiplier tubes (PMT) which are mounted on the optical table. The signal detected by PMT is processed by a TSI Inc., IFA 750 Digital Burst Correlator. More details are available in (7,8,9).

Particle Seeding

High speed flow visualization and LDV measurements depend mainly on the existence of particles in the flow to scatter enough light to obtain a high level of contrast and data rate. Visual observation results and LDV measurements can be influenced by the size distribution, concentration and light scattering efficiency of the particles suspended in the flow. Additionally, seeding particles must fulfill the following requirements: (1) ability to follow the flow; (2) no window fouling; (3) non-toxic and non-active chemically; (4) no effect on the combustion process and maintain their sizes in compression and burning gas[6].

A large number of experiments have been conducted to test reliable seeding techniques and select seeding particles from many kinds of materials to fit different experiments. Phenolic microballoon particles (40 μm mean diameter), titanium dioxide powder (0.5-2 μm), aluminum oxide powder (1-3 μm), smoke (incense), and other particles are adequate for flow visualization. Propylene glycol liquid (0.3-0.8 μm), boron nitride powder (0.2-0.7 μm), titanium dioxide powder (0.5-2 μm) and Zirconium fluoride (0.2-0.8 μm) are suitable for LDV measurements.

Steady Air Flow Induction System Assembly

The steady state induction system consists of an air filter housing and a MAFS unit used in a 3.8L engine at a flow rate of 12-525 kg/h. Parts of the system were reconstructed to make optical access through the air filter cover and MAFS unit for the flow visualization study. Because of the seams, outer support ribs and rubber connector with hose clamps on the clear plastic air filter cover and sensor unit, flow visualization would be very limited. To avoid this problem a clear one-piece plastic air filter cover and MAFS unit was constructed. The assembly includes the air filter cover through the mass air flow unit as shown in Figure 2. The rubber connector is not needed in the new assembly because a clear plastic piece was machined that simulated the connection between the mass air flow unit and the cover of the air filter. These pieces were then glued together with a clear adhesive to form a clear one-piece cover and sensor unit.

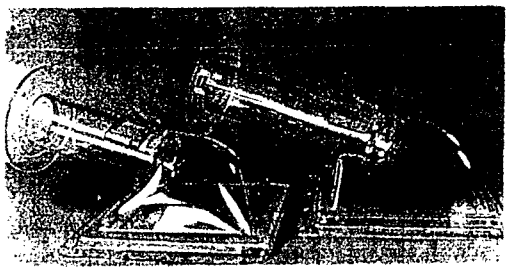

(a) Modified cover (b) Original cover

Fig. 2 Modified and original air filter covers

The cover and sensor unit was fastened to a (1.22 x 2.1 x 2.44 m) plenum. The entire assembly is shown in Figure 1. A spencer four-stage centrifugal blower was used at the opposite end of the plenum to draw air through the test assembly. The amount of air allowed to flow through the test assembly was controlled by the angle of a throttle plate located downstream from the blower. The flow rate of a given throttle angle was calibrated by mounting a

Meriam laminar air flow element (LAFE) model 50MCZ-4 upstream from the air filter assembly. The flow rate was measured by a Meriam inclined manometer model 50MC2-4 which reads the differential pressure across the LAFE and the flow rate in CFM.

Modified cover - analysis of the flow observations performed in the original cover indicated that the sharp corners of the cover next to the air filter and the sharp entry region of the main passage accounted for the high level of fluctuations generated near the bypass inlet and the subsequent flow separation occurring at the upper wall of the cover. For this reason, a new cover was designed and formed to reduce the fluctuations in the same MAFS unit.

The first modification was to move the edges of the cover on the four sides of the air filter. The cover sealed to the rubber on the air filter in the same manner, but the flange edges were brought inward enough to line up with the border of the air filter paper and rubber seal material. This modification reduced the step caused by the rubber seal and allowed air to flow through the filter with less disturbance. The second modification was to round off the two corners of the cover which are located on the opposite side from the MAFS unit. The last modification was to change the externally protruding corners on either side of the MAFS unit. Thus cover was sloped gradually up toward the main passage.

RESULTS AND DISCUSSION

A comparison of the controlling effect of the two cover designs on the turbulence structure formation, level of fluctuations and sensor output signal is presented. A series of photographs selected from 16 mm high speed motion pictures are shown and described in this section to facilitate understanding the flow patterns in an axial and radial plane.

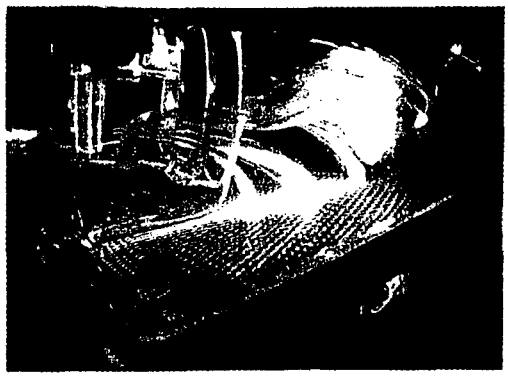

(a)

(b)

Fig. 3 Flow pattern in an axial plane passing through the bypass and main passage axes at a flow rate of 50 kg/h (a) Original cover (b) Modified cover

Figure 3(a) shows the flow development in the original cover. The view shown is of an axial plane passing through the axes of the main and bypass passage. The motion pictures showed that the turbulence flow field is markedly influenced by the air filter cover configuration and the disturbances near the wall are caused by the vortices originated near the corners of the original cover and along the edges next to the air filter. This flow pattern dominates the boundary region of the upper part of the cover and finally leads to an oscillating flow separation from the wall near the bypass. At this flow rate (50 kg/h), as observed in the experiment, the vortices originating in the corners under the main

passage curl up in concentrated spiral motions and interact with the flow stream in the axial plane passing through the axes of the bypass and main passage. For instance, in the vicinity of the bypass inlet the motion pictures revealed a high level of fluctuation which is very likely to increase the signal-to-noise ratio and disturb the sensor output signal.

Several high speed movies were recorded to analyze the flow characteristics within the original air filter cover and main passage. The original cover geometry led to a separation at the cover upper wall near the bypass inlet. This flow structure formation is a result of the interaction between the air stream flowing in the axial plane and the vortex layers springing from the corners of the cover, especially near the restricted sharp corners under the main passage inlet. Analysis of the films indicate that the instability convected downstream toward the MAFS unit is introduced by the disturbances generated in the corners of the cover, the sharp entry of the MAFS main passage, and along the edges between the cover and the rubber seal of the air filter.

In contrast, figure 3(b) presents the flow patterns in the modified cover. A significant reduction in the vortical structure formation was observed and the flow separation has disappeared at the cover upper wall. This in turn exhibited less fluctuation in the vicinity of the bypass inlet. In this respect, it seems that the air filter cover and the bypass inlet/outlet design are important factors to maintain a low level of disturbance in the sensor output voltage. The modifications made on the cover can be seen by comparing figures 3(a) and 3(b). The difference in the flow features is already apparent from this figure. For example, the flow separation and the deflection of the flow stream toward the center of the main passage in figure 3(a) are not apparent as in figure 3(b) near the upper wall of the cover.

The flow patterns in the main passage radial plane at 0.5 cm from the sensor bypass inlet are presented in figures 4(a) and 4(b) in the original and modified cover at the same flow rate of 50 kg/h. It is apparent in this plane that the covers and the entry region have a significant influence on the flow characteristics. One can observe in this plane the entry region of the MAFS and the bypass inlet, where the flow manifests itself in cylindrical vortex pairs as a consequence of the flow generated within the covers. In the original cover figure 4(a) indicates that the vortical tubes do not flow through the bypass inlet due to the flow separation and the instabilities caused by the cover. On the other hand, figure 4(b) shows steadiness in the vortical structure, also a vortical tube is stretched into the bypass inlet which will consequently reduce the disturbance at the surface of the probe.

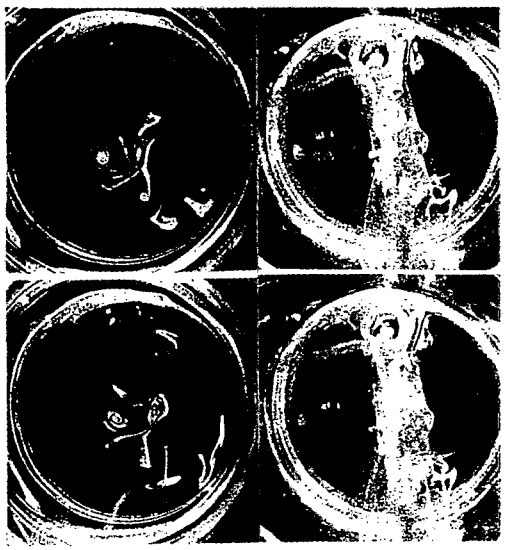

(a) Original cover (b) Modified cover

Fig. 4 Flow patterns in the main passage radial plane at 0.5 cm from the bypass at a flow rate of 50 kg/h

To quantify the flow observations illustrated in figure 4(b) (modified cover), LDV measurements

of the velocity and turbulence intensity were performed in the main passage radial plane at 2.5 cm from the bypass inlet and at a flow rate of 50 kg/h. Two velocity component were measured in this study, one component perpendicular to the measurement plane (u-component), and one component in the measurement plane perpendicular to the filter surface (v-component). On the figures, positive u-component is into the plane of the paper and positive v-component is towards the top of the page. The measurements were conducted on a grid of locations at a distance of 8 mm from each other. Figures (5 and 6) show the velocity variations, which are related to the fluctuations seen in the motion pictures and the unsteady vortical structure. On the top and bottom of these figures, the measurement locations are closer to the inner surface of the assembly than the locations on the sides. This is a result of being able to measure nearer the walls in these locations due to the geometrical orientation of the assembly.

Figure 5 represents the u-component normalized mean velocity and standard deviation in m/s for 50 kg/h. The velocities are higher on the sides when compared to the central portion of the graph. This may be due to the bypass passage stagnation region having an influence on the flow at the measurement location. But, figure 5(a) shows almost uniform velocity distribution over a large fraction of the region of interest. Larger velocity gradients are also seen on the top and bottom of the graphs. The flow characteristics here result from separation and resultant turbulence generated near the wall at the entrance to the MAFS assembly.

Figure 6 represents the v-component normalized mean velocity and standard deviation in m/s for 50 kg/h. The v-component velocities decrease from the bottom to the top of the graph. The standard deviation graphs show the upper region to be substantially less turbulence than the lower region. This is attributed to the separating flow at the lower edge of the main passage.

Finally, figure 7 illustrates a comparison of the noise test results with the original and modified cover/MAFS assembly. This data shows noise on the ordinate as a function of the mass flow rate over a range of 12-525 kg/h. A noise reduction of 15 % at 12 kg/h and 65 % at 525 kg/h were measured.

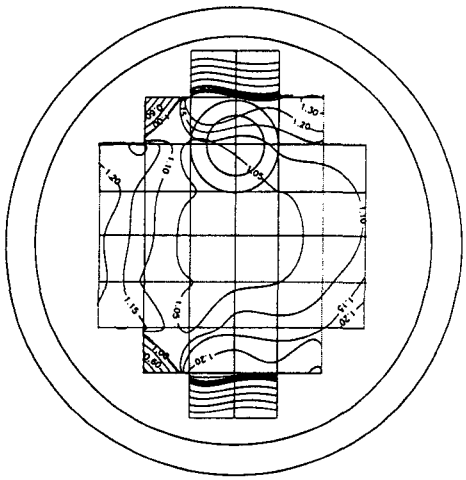

(a) Normalized mean velocity

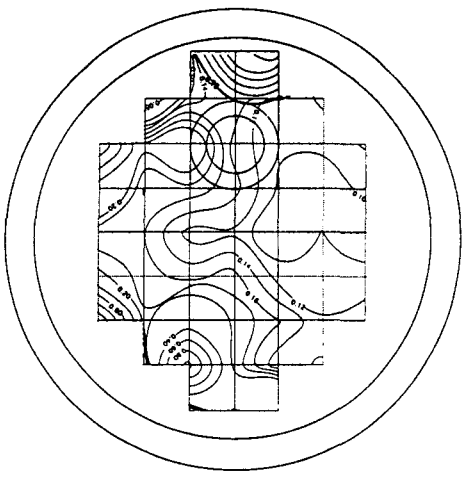

(b) Standard deviation

Fig. 5 Normalized mean velocity and standard deviation in m/s for 50 kg/h (u-component)

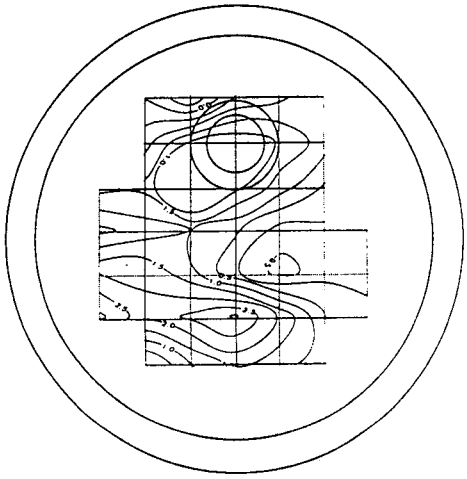

(a) Normalized mean velocity

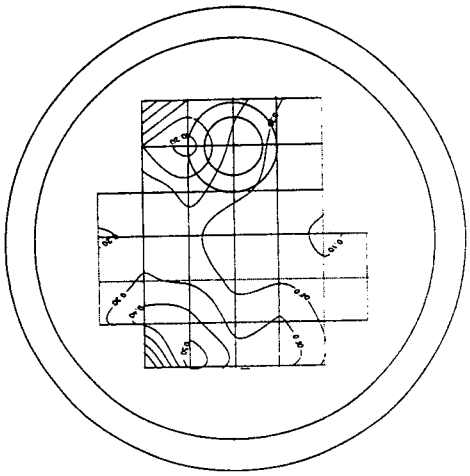

(b) Standard deviation

Fig. 6 Normalized mean velocity and standard deviation in m/s for 50 kg/h (v-component)

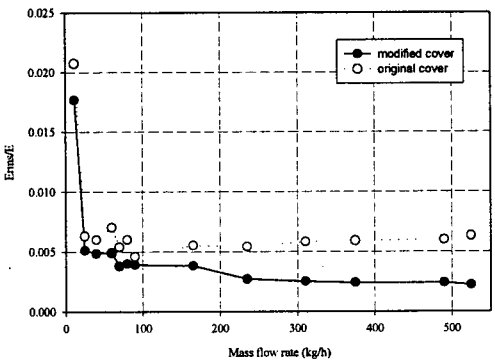

Fig. 7 Test result on noise

CONCLUSION

Flow visualization and LDV mapping within an air filter cover and main passage of an air induction system were presented to analyze the flow behaviors and its effect on the sensor performance. The following conclusions can be drawn based on the results of this study.

1) Several important characteristic flow features have been observed. They include the unstable oscillations of the flow field in the vicinity of the MAFS bypass passage, air cleaner upper cover edge effects, and the rotating air stream near the air cleaner corners which influenced markedly the flow behaviors in the main passage. This provided valuable information to interpret how cover/bypass concepts can affect the flow pattern and the sensor performance.

2) In the experiments vortical structure was observed near the central portion of the main passage. The nature of this structure is believed to be related to the 90 degree flow turning in the system.

3) In the original cover the simultaneous interaction of the sharp corners, entry region and the edges between the cover and the air filter rubber seal produced a complex flow field and consequently a high level of signal-to-noise ratio in the sensing element output.

4) In the modified cover the experimental data demonstrated a substantial decrease in the turbulence fluctuations and the output signal-to-noise level.

5) Small geometrical differences in the induction system have been seen to influence the flow characteristics in the MAFS assembly.

6) Comparison of this experimental result with the predicted result from CFD will be a good tool to design for the air induction systems.

REFERENCES

1. W.G.Wolber, "Automotive Engine Control Sensor 80,"SAE Paper No. 800121, 1980

2. R.Sauer, "Automotive Air Flow Measurement," Proceedings of the International Symposium on Automotive Technology and Automation (ISATA), Volume 1, pp. 91-106, Wolfsburg, W.Germany, 1978

3. A. Zias, "A New Approach to Flowmetering - Simple Mechanical Device Allows Use of Reasonably Specified Pressure Transducer for Flow and Total Volume Metering," SAE Paper No. 760019, 1976

4. R. Dell'Aqua and P. Vicini, "Ultrasonic Transducers for an Automotive Air Flow Meter," Presented at the First ISATA Sensor Study Group Meeting, Rome, Italy,4/29-4/30 1979

5. R. Schledde, "Konstant-Temperatur-Anemomet er," Messen und Pruefen/Automatik, pp. 679-683, 1980

6. Regan, C.A., Chun, K.S. and Schock, H.J., "Engine Flow Visualization Using Copper Vapor Laser," Proceedings of SPIE, Vol. 737, pp. 17-27, 1987

7. Lee, k., Yoo, S.-C., Steucken, T., McCarrick, D., and Schock, H.J., "An Experimental Study of In-Cylinder Air Flow in a 3.5L Four Valve SI Engine by High Speed Flow Visualization and Two-Components LDV Measurement," SAE 930478, 1993

8. Yoo, S.-C., Lee, k., Novak, M., and Schock, H.J., "3-D LDV Measurement of In-Cylinder Air Flow in a 3.5L Four Valve SI Engine," SAE 95648, 1995

9. Hascher, H., Novak, M., Lee, k., Schock, H.J., Rezaei, H., Koochesfahani, M., "An Evaluation of IC-Engine Flows with the Use of Modern In-Cylinder Measuring Techniques,"34th AIAA / ASME/SAE/ASEE Joint Propulsion Conference & Exhibit, July 13-15, 1998, Cleveland, OH